Regulation of GABAergic synapse formation and plasticity by GSK3β-dependent phosphorylation of gephyrin

Shiva K. Tyagarajan[a,1], Himanish Ghosh[a], Gonzalo E. Yévenes[a], Irina Nikonenko[b], Claire Ebeling[a], Cornelia Schwerdel[a], Corinne Sidler[a], Hanns Ulrich Zeilhofer[a], Bertran Gerrits[c], Dominique Muller[b], and Jean-Marc Fritschy[a]

[a]Institute of Pharmacology and Toxicology, University of Zurich, CH-8057 Zurich, Switzerland; [b]Département des Neurosciences Fondamentales, Centre Médical Universitaire, CH-1211 Geneva 4, Switzerland; and [c]Functional Genomics Center Zurich, CH-8057 Zurich, Switzerland

Edited by Richard L. Huganir, The Johns Hopkins University School of Medicine, Baltimore, MD, and approved November 30, 2010 (received for review August 11, 2010)

Postsynaptic scaffolding proteins ensure efficient neurotransmission by anchoring receptors and signaling molecules in synapse-specific subcellular domains. In turn, posttranslational modifications of scaffolding proteins contribute to synaptic plasticity by remodeling the postsynaptic apparatus. Though these mechanisms are operant in glutamatergic synapses, little is known about regulation of GABAergic synapses, which mediate inhibitory transmission in the CNS. Here, we focused on gephyrin, the main scaffolding protein of GABAergic synapses. We identify a unique phosphorylation site in gephyrin, Ser270, targeted by glycogen synthase kinase 3β (GSK3β) to modulate GABAergic transmission. Abolishing Ser270 phosphorylation increased the density of gephyrin clusters and the frequency of miniature GABAergic postsynaptic currents in cultured hippocampal neurons. Enhanced, phosphorylation-dependent gephyrin clustering was also induced in vitro and in vivo with lithium chloride. Lithium is a GSK3β inhibitor used therapeutically as mood-stabilizing drug, which underscores the relevance of this posttranslational modification for synaptic plasticity. Conversely, we show that gephyrin availability for postsynaptic clustering is limited by Ca^{2+}-dependent gephyrin cleavage by the cysteine protease calpain-1. Together, these findings identify gephyrin as synaptogenic molecule regulating GABAergic synaptic plasticity, likely contributing to the therapeutic action of lithium.

$GABA_A$ receptors | lithium chloride | postsynaptic density | PSD95 | homeostatic plasticity

Plasticity of chemical synapses endows neuronal networks with the capacity to store information by adjusting their functional connectivity. Hence, understanding the molecular underpinnings of synaptic plasticity is a fundamental quest of neuroscience. These mechanisms have been characterized most extensively at glutamatergic synapses, in which a core scaffolding protein, PSD95, forms a signaling complex assembled by proteins interacting via specific PDZ domains (1). In contrast, little is known about signals regulating GABAergic synapses, despite their ubiquitous presence throughout the CNS and their key role in the control of network activity and synchronization. In particular, the postsynaptic density (PSD) of GABAergic synapses, localized primarily on neuronal somata and dendritic shafts, remains ill characterized. Gephyrin, a 93-kDa cytoplasmic polypeptide, has emerged as a multifunctional protein mediating postsynaptic aggregation of $GABA_A$ receptors ($GABA_AR$) and glycine receptors by forming a scaffold anchored to the cytoskeleton (2–4). However, the mechanisms of gephyrin and $GABA_AR$ clustering are poorly understood, although evidence for direct interaction between gephyrin and $GABA_AR$ is slowly emerging (5, 6). Though gephyrin is a phosphoprotein (7, 8), the relevance of gephyrin phosphorylation for regulating GABAergic transmission has not been addressed.

In the present work, we focused on gephyrin posttranslational modification for regulating its postsynaptic clustering and stability. Considering the importance of PSD95 phosphorylation for trafficking in dendritic spines and regulating glutamate receptor postsynaptic localization (9, 10), we used a multidisciplinary approach to elucidate protein kinase pathways controlling gephyrin clustering at GABAergic synapses. We report the identification and biochemical characterization of a unique phosphorylation site on gephyrin, Ser270, which is targeted by glycogen synthase kinase 3β (GSK3β) to modulate GABAergic transmission. We assessed the effects of transient expression of phosphodeficient and phosphomimicking gephyrin constructs in cultured hippocampal neurons on gephyrin clustering at postsynaptic sites and on frequency of miniature GABAergic postsynaptic currents. The pharmacological relevance of GSK3β activity was determined by analyzing the effects of the mood-stabilizing drug lithium, a well-characterized GSK3β inhibitor, on gephyrin clustering at GABAergic synapses and on its ability to influence inhibitory/excitatory balance by concerted modulation of PSD95 clustering in glutamatergic synapses. Finally, we investigated the role of Ca^{2+}-dependent proteolysis by calpain-1 in controlling gephyrin stability and availability for postsynaptic clustering upon changes in Ser270 phosphorylation status.

Results

Identifying Unique Phosphorylation Sites on Gephyrin. Using tandem mass spectrometry (MS/MS) analysis of native gephyrin isolated from adult mouse brain homogenate by immunoprecipitation, we identified a phosphopeptide, with Ser270 as a unique phosphorylation site (*Materials and Methods*). To study the relevance of Ser270 phosphorylation for gephyrin postsynaptic clustering, we introduced point mutations in eGFP-gephyrin to create S270A (phosphorylation defective) and S270E (phosphorylation mimicking) mutants. These constructs were transfected in cultured neurons after 11 d in vitro (DIV) and analyzed 7 d later (11 + 7 DIV) by confocal microscopy, quantifying the size and number of postsynaptic clusters formed by eGFP-gephyrin S270A and S270E mutants on 20-μm length dendrites of transfected neurons. We have shown previously (11) that this approach leads to correct targeting of eGFP-gephyrin and allows quantitative assessment of

Author contributions: S.K.T. designed research; S.K.T., H.G., G.E.Y., I.N., C.E., C. Schwerdel, C. Sidler, and B.G. performed research; S.K.T., H.G., G.E.Y., I.N., H.U.Z., D.M., and J.-M.F. analyzed data; and S.K.T. and J.-M.F. wrote the paper.

The authors declare no conflict of interest.

This article is a PNAS Direct Submission.

Freely available online through the PNAS open access option.

[1]To whom correspondence should be addressed. E-mail: tyagarajan@pharma.uzh.ch.

This article contains supporting information online at www.pnas.org/lookup/suppl/doi:10.1073/pnas.1011824108/-/DCSupplemental.

gephyrin clusters at postsynaptic sites, identified by apposition to synapsin-1-positive presynaptic terminals.

Neurons expressing the S270A mutant had an increased number of gephyrin clusters compared with WT eGFP-gephyrin (18.1 ± 1 per 20-μm dendrite segment vs. 7 ± 0.5; Fig. 1 *A* and *B* and Table S1), unchanged in size (Fig. 1*C*), whereas expression of S270E produced no significant effect. As a control, we observed that postsynaptic clusters formed by gephyrin S270A mutant still colocalized with the $GABA_AR$ α2 subunit (Fig. 1 *D* and *D′*). These observations suggested that dephosphorylation of gephyrin at Ser270 facilitates postsynaptic cluster formation.

To test whether endogenous gephyrin influenced these phenotypes, neurons were cotransfected with a shRNA targeting the *GEPHN* mRNA 3′UTR to deplete endogenous gephyrin without affecting expression of eGFP-constructs (which lack the 3′UTR), as reported earlier (12). To demonstrate its specificity, we used the shRNA with three point-mutations in its sequence (3′UTR-3m). Cells were analyzed after 11 + 7 DIV by triple-fluorescence with a presynaptic marker (Fig. 1 *E–I*). Depletion of endogenous gephyrin was effective (Fig. 1 *E* and *F*) but did not prevent formation of supernumerary S270A postsynaptic clusters (Fig. 1 *G* and *I*). Down-regulation of endogenous gephyrin had no significant effect on S270E postsynaptic clusters (Fig. 1 *H* and *I*) when compared with eGFP-gephyrin (Fig. 1*I* and Table S1).

Functional Analysis of Gephyrin Ser270 Phosphorylation Mutants. Next, to assess the functional relevance of Ser270 phosphorylation, whole-cell patch-clamp recordings of miniature inhibitory postsynaptic currents (mIPSCs) were performed. Overexpression of WT eGFP-gephyrin did not influence mIPSC amplitudes or interevent intervals compared with mock-transfected cells present on the same coverslip (Fig. 2 and Table S2), indicating that recombinant gephyrin did not cause measurable overexpression artifacts. In contrast, the average amplitude of mIPSCs recorded in neurons expressing S270A was 10% larger than control (Fig. 2*B*), and the interevent intervals were shortened by 25% (Fig. 2*B*

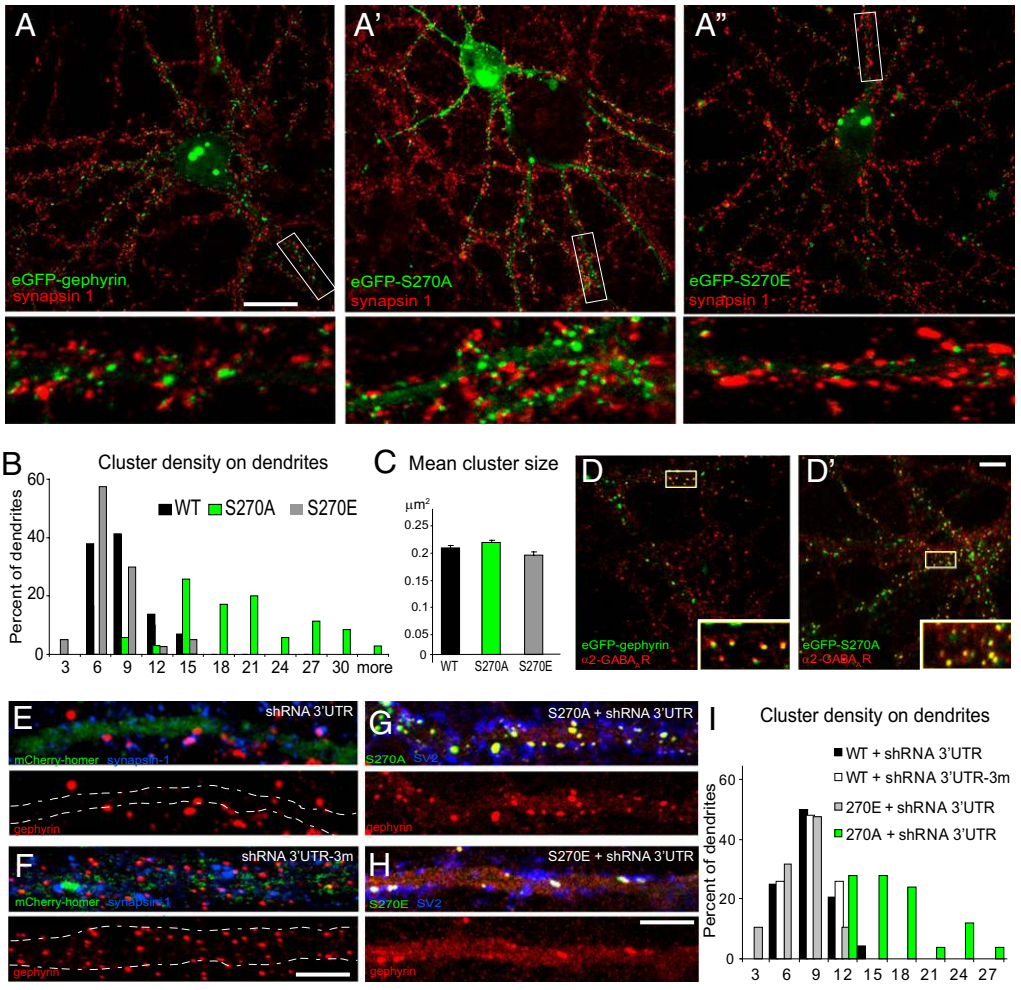

Fig. 1. Morphological analysis of gephyrin phosphorylation-site mutants. (*A–A″*) Typical examples are illustrated for each mutant construct; postsynaptic clustering is demonstrated by apposition of eGFP-gephyrin clusters (green) to synapsin-1-positive terminals (red). (Scale bar: 20 μm.) (*B*) Distribution of postsynaptic cluster density for WT and individual eGFP-gephyrin mutants on dendrites of transfected neurons (normalized to 20-μm segments); a significant increase is evident for the S270A mutant. (*C*) No significant change in mean cluster area was observed in S270A or S270E mutants compared with WT eGFP-gephyrin. (*D* and *D′*) Clusters formed by eGFP-gephyrin and S270A mutant colocalize with the α2 subunit, confirming their interaction with $GABA_AR$. (Scale bar: 10 μm.) (*E* and *F*) Endogenous gephyrin (red) depletion in cells cotransfected with shRNA targeting the *GPHN* 3′UTR and mCherry-homer (green; to visualize the transfected dendrites). Presynaptic terminals were stained with synapsin-1 (blue). The residual gephyrin clusters are present in nontransfected cells. (*F*) Gephyrin is not affected by cotransfection of shRNA 3′UTR containing three point-mutations (3m) as control. (Scale bar: *E* and *F*, 5 μm.) (*G* and *H*) Representative images of S270A and S270E constructs cotransfected with gephyrin shRNA 3′UTR. (Scale bar: 5 μm.) (*I*) Quantification of cluster density per 20-μm dendritic length shows that down-regulation of endogenous gephyrin does not alter the S270A and S270E phenotypes (cf. Fig. 1*B*). See Table S1 for statistical analysis.

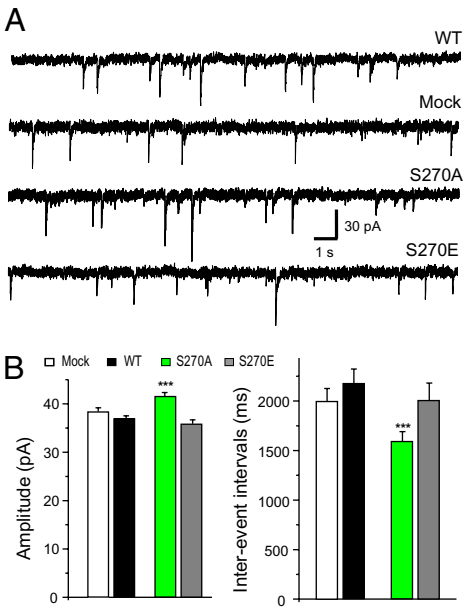

Fig. 2. Effects of WT and mutant eGFP-gephyrin expression on GABAergic mIPSCs. (*A*) Representative current traces show pharmacologically isolated GABAergic mIPSCs recorded at 11+ 4 DIV for the constructs tested and nontransfected neurons from the same coverslips (mock). (*B*) Histograms show average amplitude and interevent intervals of mIPSCs recorded under each experimental condition. Bars indicate mean ± SEM of 500–1,500 mIPSCs per condition, obtained from 9–14 neurons. The decreased interevent intervals between mIPSCs observed with S270A reflects the corresponding increase gephyrin cluster density seen morphologically. See Table S2 for statistical analysis. ***$P < 0.001$ compared with WT eGFP-gephyrin.

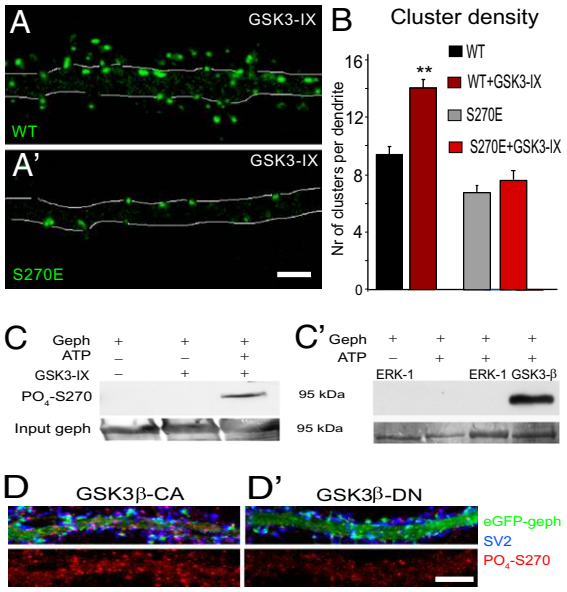

Fig. 3. GSK3β phosphorylates gephyrin at Ser270. (*A* and *B*) Overnight exposure to GSK3-IX (5 μM) enhances eGFP-gephyrin cluster density (*A*) in 11 + 7 DIV transfected cells but does not affect the corresponding S270E mutant construct (*A′*), as shown with representative examples and quantitative analysis (*B*); see Table S1 for statistics. (*C*) In vitro phosphorylation of gephyrin by purified GSK3β, and detected using a polyclonal antibody against phospho-Ser270. The gephyrin band was detected only in the presence of the kinase and ATP (lane 3), even though stripping the blot and reprobing with (monoclonal 3B11) shows same amounts of full-length gephyrin in all lanes. (*C′*) In vitro phosphorylation of gephyrin using purified ERK-1 and Western blot using phospho-S270 gephyrin antibody showed gephyrin band only in the positive control GSK3β lane (lane 4). The blots were later stained with Coomassie blue to check gephyrin amounts (*Lower*). (*D* and *D′*) Enhanced detection of phosphorylated gephyrin clusters using anti–phospho-Ser270 antibody (red) in cultured neurons coexpressing eGFP-gephyrin (green) with GSK3β-CA (*D*) but not GSK3β-DN (*D′*); presynaptic terminals were labeled with SV2 (blue). (Scale bars: 2 μm.)

and Table S2), suggesting increased density of functional GABAergic synapses. In cells transfected with S270E mutant, mIPSCs were similar to WT or mock-transfected cells, reflecting the results of Fig. 1. Finally, the rise and decay time constants of mIPSCs did not change appreciably (Fig. S1), suggesting no differences in localization or functional properties of $GABA_AR$ in transfected neurons. Thus, constitutive blockade of gephyrin Ser270 phosphorylation allows formation of supernumerary, functional GABAergic synapses in cultured neurons.

Identifying the Kinase Pathway Regulating Ser270 Site in Gephyrin. We tested different protein kinase inhibitors for their effect on gephyrin clustering, expecting proline-directed serine/threonine kinases to be effective, as a proline residue flanks Ser270 (DTASLSTTPSEsPR). Accordingly, overnight treatment of neuronal cultures with inhibitors of the non–proline-directed kinases PKA (H-89, 5 μM; KT5720; 1 μM) and PKC (calphostin C; 2 μM) had no observable effect on eGFP-gephyrin clustering. However, overnight exposure to the GSK3β inhibitor GSK3-IX (5 μM) induced a marked increase in postsynaptic eGFP-gephyrin cluster density (Fig. 3 *A* and *B* and Table S1), mimicking the phenotype of the S270A mutant. In control experiments, GSK3-IX exposure did not modify the phenotype of eGFP-S270E mutant (Fig. 3 *A′* and *B* and Table S1), confirming the selectivity of GSK3β action on Ser270. As seen in Table S1, the size of WT and S270E gephyrin clusters was significantly reduced by GSK3-IX, suggesting that GSK3β inhibition limits gephyrin availability.

To provide independent evidence for GSK3β-mediated phosphorylation of gephyrin at Ser270, we used in vitro kinase assay and Western blotting with a Ser270 phosphorylation-specific antibody (Fig. 3*C*). In this assay, we incubated purified bacterially expressed recombinant gephyrin (to avoid contamination with other kinases) with active form of purified GSK3β. As shown by Western blotting (Fig. 3*C*), a phosphorylation-specific band was detected only in the presence of ATP, suggesting that gephyrin might be a direct substrate for GSK3β. To test the specificity of our antibody and phosphorylation of S270 by GSK3β, we performed in vitro kinase assay using another proline-directed kinase, ERK1. Western blot using our gephyrin S270 phosphorylation-specific antibody shows a gephyrin-positive band only in our positive control GSK3β (Fig. 3*C′*). In addition, we confirmed GSK3β-mediated gephyrin phosphorylation in neurons by cotransfecting eGFP-gephyrin with either a constitutively active (CA) or dominant negative (DN) GSK3β mutant. Labeling of postsynaptic eGFP-gephyrin clusters with anti–phospho-S270 antibody at 11 + 7 DIV demonstrated that gephyrin is phosphorylated at Ser270 in the presence of GSK3β-CA, but not GSK3β-DN (Fig. 3 *D* and *D′*).

Lithium Chloride (LiCl) Exposure Increases Gephyrin Clustering. To explore the relevance of GSK3β inhibition for modulating GABAergic synaptic transmission, we tested the effect of the mood-stabilizing drug lithium on gephyrin clustering, because of its well-known inhibition of GSK3β activity. Overnight exposure of transfected neurons to LiCl (2, 10, and 20 mM) at 11 + 7 DIV significantly increased the density of postsynaptic eGFP-gephyrin clusters compared with neurons exposed to NaCl (from 7 ± 0.5–15.9 ± 1.1 clusters per 20-μm dendrite segment; Fig. 4 *A* and *B* and Table S1). Next, we tested whether Ser270 phosphorylation underlies these effects of lithium. In neurons transfected with

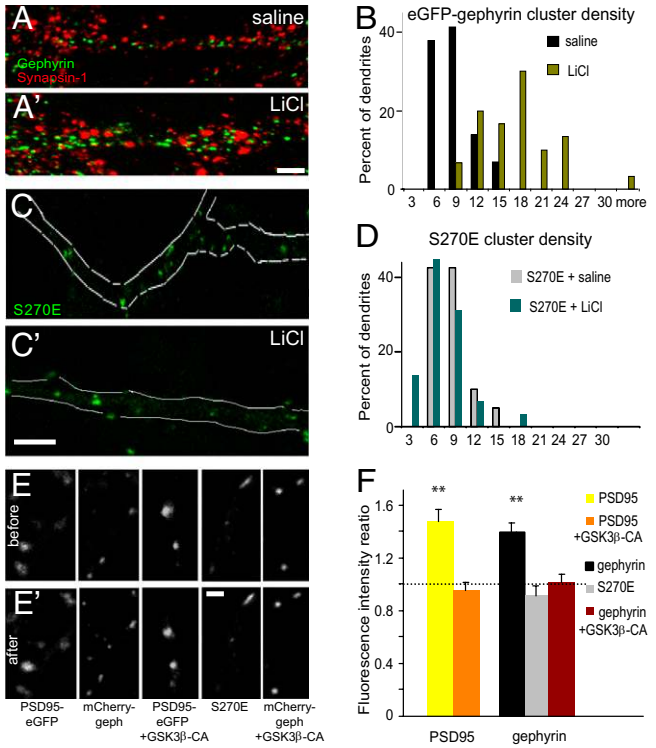

Fig. 4. LiCl affects postsynaptic gephyrin clusters in cultured hippocampus neurons. (*A* and *B*) Increased density of eGFP-gephyrin clusters (green) apposed to synapsin-1-positive terminals upon overnight exposure to 20-mM LiCl, as shown in representative examples and upon quantification. (*C* and *D*) LiCl treatment does not affect the phenotype of S270E mutant. See Table S1 for average values and statistical analysis. (*E*) Changes in mCherry-gephyrin and PSD-95-eGFP clustering in organotypic hippocampal cultures after LiCl treatment. Repeated images of dendritic segments of transfected CA1–CA3 pyramidal neurons in organotypic cultures were taken before and after 7-h exposure to 20-mM LiCl. (*F*) Quantitative analysis (mean ± SEM) of the size of fluorescent puncta measured as integrated fluorescence intensity and expressed as ratio of values obtained for the same clusters after/before LiCl treatment. The data include effects of LiCl on PSD95-eGFP (n = 5 cells; 98 clusters; $^{**}P < 0.0001$), PSD95-eGFP cotransfected with GSK3β-CA (n = 4 cells; 75 clusters; $P > 0.4$), mCherry-gephyrin (n = 5; 70 clusters; $^{**}P < 0.0001$), S270E (n = 6 cells; 57 clusters; $P > 0.2$), and mCherry-gephyrin cotransfected with GSK3β-CA (n = 4 cells; 61 clusters; $P > 0.7$). (Scale bars: 2 μm.)

S270E mutant, no effect on gephyrin cluster density was observed after 12-h exposure to 20-mM LiCl (Fig. 4 *C* and *D* and Table S1), confirming the specificity of lithium inhibition of GSK3β. However, as observed above with GSK3-IX, the size of clusters was reduced (Table S1), indicating that enlargement of eGFP-gephyrin clusters after LiCl exposure involves an additional mechanism.

To assess possible in vivo effects of lithium on GABAergic synapses, we examined the effects of chronic LiCl administration in adult mice over 72 h on gephyrin cluster and GABAergic presynaptic terminal density in four brain regions (Fig. S2 *A–E*). In addition, we investigated possible alterations at glutamatergic synapses by analyzing PSD95 clusters (Fig. S3 *A–C*). Double-immunofluorescence staining revealed region- and synapse-specific effects of LiCl treatment, in particular a significant increase in gephyrin cluster density in the hippocampal formation, as well as 25% increase in the density of GABAergic terminals selectively in the molecular layer of the dentate gyrus (Table S3). Only a small fraction of gephyrin clusters were not apposed to $vGAT^+$ terminals (4–17% total gephyrin clusters/section); this proportion did not change after chronic LiCl treatment (Fig. S2 *A′–C′*, arrows), confirming detection of synaptic sites. In addition, lithium had different effects on the size of gephyrin clusters in the four regions analyzed (Fig. S2*E*). Interestingly, these pre- and postsynaptic alterations of GABAergic synapses were mirrored by an increase in size, but not density, of PSD95 clusters in the corresponding regions (CA1, dentate gyrus, cerebral cortex; Fig. S3 *B* and *C* and Table S3), suggesting a compensatory response to maintain excitatory/inhibitory balance.

To search for a mechanistic link between GSK3β-mediated phosphorylation of gephyrin and dynamic regulation of GABAergic/glutamatergic postsynaptic scaffolds, we tested the effect of lithium on gephyrin and PSD95 clustering using confocal imaging in organotypic slices cotransfected with PSD95-eGFP and mCherry-gephyrin. Selected regions of interest were imaged before and after a 7-h exposure to LiCl to determine the variations in size of single clusters by measuring their integrated fluorescence intensity. On average, a 40% increase in fluorescence intensity of identified PSD95 or gephyrin clusters was detected upon LiCl exposure (Fig. 4 *E* and *F*). In neurons cotransfected with GSK3β-CA mutant, LiCl treatment was ineffective in altering the fluorescence intensity of PSD95 or gephyrin clusters. Likewise, lithium had no effect upon expression of gephyrin S270E mutant (Fig. 4*F*). Therefore, it is likely that lithium affects both gephyrin and PSD95 clustering via the regulation of GSK3β activity at GABAergic and glutamatergic synapses.

Gephyrin Clusters Are Regulated by Activated Calpain-1 and Calpastatin. No molecular mechanism has been proposed so far to explain gephyrin turnover at postsynaptic sites. Gephyrin S270E clustering is reduced compared with S270A and cannot be rescued by inhibition of GSK3β, suggesting phosphorylation-dependent impairment of gephyrin stability or oligomerization properties. To address these possibilities, we reasoned that an activity- and/or Ca^{2+}-dependent protease might represent an attractive candidate for rapid and locally controlled removal of gephyrin. Among possible candidates involved in synaptic plasticity (13), we considered calpain-1, which is a Ca^{2+}-dependent cysteine protease highly expressed in the brain (reviewed in refs. 14 and 15). It regulates glutamatergic transmission by acting on PSD95 and NMDA receptors (16–18). Furthermore, gephyrin is a substrate for calpain-1 in the brain (19).

First, we tested whether calpain-1 cleaves native gephyrin in vitro. Addition of Ca^{2+} and purified calpain-1 to cytoplasmic or membrane-associated fractions of mouse hippocampus resulted in effective gephyrin proteolysis, whereas Ca^{2+} or purified calpain-1 alone had no effect (Fig. 5*A*). These findings indicated that the entire pool of gephyrin is potentially susceptible to proteolysis by Ca^{2+}-activated calpain-1. Next, to determine whether calpain-1 directly interacts with gephyrin, we performed immunoprecipitation of Flag-gephyrin and HA-calpain-1 coexpressed in HEK293 cells. By Western blot analysis we detected an interaction between the two proteins, selectively involving the gephyrin E-domain (Fig. 5 *B* and *B′*). Furthermore, triple-transfection experiments showed that though coexpression of GSK3β or its CA or DN mutants affected gephyrin Ser270 phosphorylation, it had no bearing on calpain-1 binding (Fig. S4). Finally, we found no direct interaction between Flag-gephyrin and myc-calpastatin (myc-CAST), an endogenous inhibitor of calpain-1 (20) in this assay (Fig. 5*B″*).

Based on these findings, we examined whether gephyrin clustering is regulated by calpain-1 activity. Because CAST is a potent endogenous inhibitor of calpain-1, we cotransfected primary neurons with myc-CAST and eGFP-gephyrin to constitutively block calpain-1. This condition led to increased gephyrin postsynaptic cluster density (Fig. 5 *C–E* and Table S1), and, when tested with anti–phospho-Ser270 antibody, to a marked increase in phosphorylated gephyrin in postsynaptic clusters (Fig. S5). Strikingly, coexpression of eGFP-gephyrin S270E mutants

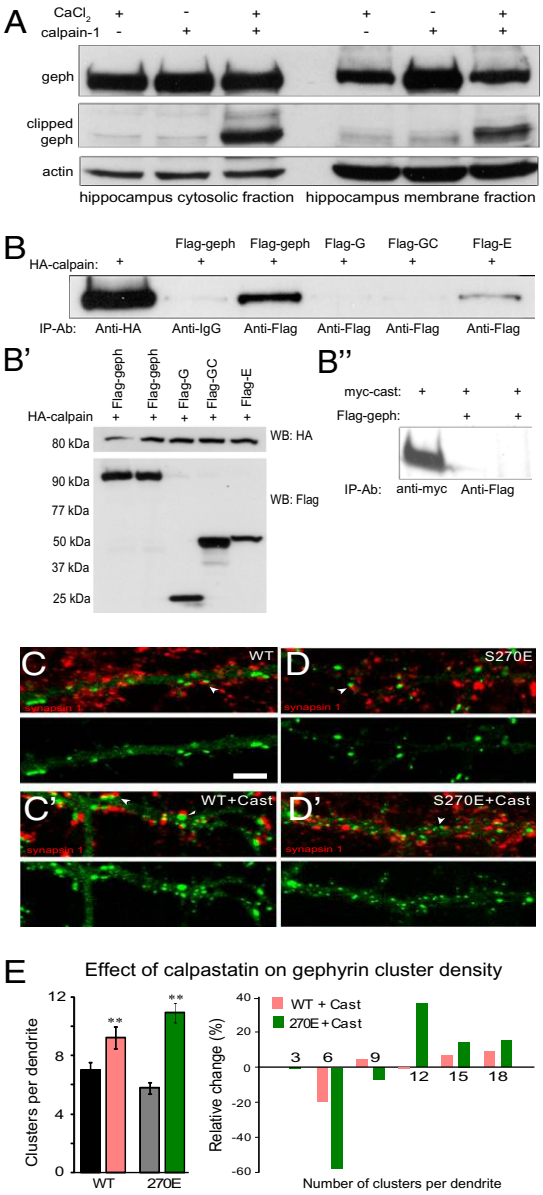

Fig. 5. Calpain-1 activity influences gephyrin clustering. (*A*) Gephyrin proteolysis by activated calpain-1, as shown by incubating cytosolic or membrane extracts of mouse hippocampal tissue with 1 μg/μL purified calpain-1 in the presence or absence of $CaCl_2$, followed by Western blot for gephyrin. (*B*) Interaction between gephyrin and calpain-1. Immunoprecipitation with antibodies against Flag from crude extracts of HEK293 cells cotransfected with Flag-gephyrin and HA-calpain-1 (lanes 1–3). Cotransfection of Flag-tagged individual gephyrin G, GC, or E domains with HA-calpain1 (lanes 4–6) demonstrates that the interaction site is located in the E domain. (*B′*) Expression levels of individual proteins in transfected HEK cells. (*B″*) No binding is detected between Flag-gephyrin and myc-CAST under similar assay conditions. (*C* and *C′*) Coexpression of myc-CAST with eGFP-gephyrin or S270E in cultured hippocampal neurons (11 + 7 DIV) increases postsynaptic gephyrin clustering to the same level as seen in cells expressing S270A. Representative panels of transfected dendrites double-labeled with synapsin-1 (red) to confirm postsynaptic localization of eGFP-gephyrin clusters (arrowheads) are shown. (Scale bar: 2 μm.) (*D* and *E*) Quantification of the average cluster density confirmed the effect of myc-CAST on both WT and S270E clusters, reflected by a shift to the right in the distribution of cluster density. See Table S1 for average values and statistical analysis.

with myc-CAST restored clustering to a level similar to S270A mutant (Fig. 5*E′* and Table S1). These findings suggest that gephyrin turnover under the control of Ser270 phosphorylation and calpain-1 activity is a key determinant of gephyrin cluster density. Remarkably, CAST coexpression had no effect on gephyrin S270E cluster size (Table S1), confirming that cluster size and number are regulated by separate mechanisms.

Finally, to show that LiCl treatment in mice blocks gephyrin Ser270 phosphorylation and calpain-1 clipping of gephyrin, we analyzed for Ser270-phosphorylated gephyrin in membrane fractions from mice chronically injected with LiCl or NaCl (Fig. S6). A small fraction of full-length phospho-gephyrin immunoreactivity was detectable in both LiCl and NaCl groups (compared with total full-length gephyrin). However, in NaCl-treated mice a large amount of clipped phospho-gephyrin fragments were immunoprecipitated, which were absent from the LiCl-treated mice (Fig. S6). This finding suggested that blocking GSK3β in vivo reduces degradation of phospho-gephyrin associated with the membrane fraction in neurons.

Discussion

In this report we demonstrate that protein phosphorylation modulates GABAergic synaptic transmission in the CNS by targeting an identified gephyrin residue, thereby modifying its postsynaptic scaffolding properties. Specifically, inhibition of GSK3β-mediated phosphorylation of gephyrin-Ser270 can induce GABAergic synaptogenesis, whereas Ca^{2+}-dependent proteolysis of gephyrin by calpain-1 limits its availability for postsynaptic clustering. Therefore, signaling cascades converging onto protein kinases and proteases regulate synapse function and homeostasis in the CNS by modifying scaffolding proteins in the PSD.

Studies of bidirectional synaptic plasticity have shown that long-lasting changes in glutamatergic synaptic function involve phosphorylation cascades targeting PSD95 (10, 21). Mechanistically, these alterations have to be paralleled by concomitant changes at GABAergic synapses to prevent hyperexcitability or silencing of the network. We now show that such effects can be achieved by protein kinases such as GSK3β, acting in concert on both gephyrin and PSD95. Mood-stabilizing drugs, including lithium and valproate, are often considered plasticity enhancers, leading upon chronic treatment to an increase in gray matter volume, possibly due to increased synaptic density (22, 23). Our data extend this view by demonstrating that changes in connectivity upon chronic LiCl administration to adult mice primarily involve GABAergic synapses.

The formation of supernumerary synapses in cells expressing phosphorylation-deficient S270A mutant, demonstrated morphologically and functionally, indicates that a single phosphorylation site on gephyrin can regulate synaptogenesis, presumably by helping to recruit other proteins that define the GABAergic PSD and thereby promoting interaction with presynaptic terminals to form functional synapses. Recently, it was demonstrated that new GABAergic synapses are formed exclusively on preexisting axon-dendritic crossings, without the involvement of dendritic or axonal protrusions (24), suggesting that fundamentally different mechanisms underlie glutamatergic and GABAergic synapse formation. Activation of intracellular signals to modify gephyrin-scaffolding properties and interaction with other synaptogenic molecules could facilitate axon-dendritic GABAergic synapse formation.

Gephyrin-interacting protein neuroligin-2 (NL2) has been selectively localized at the GABAergic synapses (25) and is an important molecule for synapse formation by means of interaction with presynaptic neurexins (26). Recently, it was suggested that NL2 is required for GABAergic synapse formation at perisomatic sites (27). Hence, understanding whether and how dephosphorylation of gephyrin-Ser270 regulates NL2 and/or CB interaction might highlight a crucial step in the formation of inhibitory synapses.

Synapse elimination has been proposed as a mechanism of activity-dependent regulation of inhibition (28). Here, we identify gephyrin proteolysis as a unique mechanism limiting the number of functional inhibitory synapses. The importance of calpain-1 activity in this process is underscored by the rescue of the S270E phosphomutant when cotransfected with calpain-1 inhibitor, CAST. Gephyrin contains two PEST sequences, one of which (residues 259–271) coincides with the phosphopeptide identified here (29). Therefore, gephyrin phosphorylation might induce a conformational change exposing the PEST sequence for calpain-1–mediated elimination of clusters. This is supported by the fact that coexpression of phosphomimicking S270E mutant with myc-CAST leads to an increased number of gephyrin clusters (Fig. S5). Importantly, the need for concomitant Ca^{2+} to activate calpain-1 provides a regulatory mechanism to spatially constrain its action, possibly allowing down-regulation of GABAergic transmission in a synapse-specific manner.

In summary, our data offers a mechanistic basis for regulating gephyrin-containing GABAergic synapses in the context of homeostatic plasticity and contributing to the action of drugs, such as lithium, that act by blocking signal transduction path ways converging onto GABAergic and glutamatergic PSDs. The ability of specific kinase pathways to mediate cross-talk between excitatory and inhibitory transmission, in concert with Ca^{2+} signals, reflects an efficient mechanism to modulate network activity.

Materials and Methods

Gephyrin isolation, MS/MS analysis of phosphopeptides, and all biochemical experiments are described in *SI Materials and Methods*, along with details of the procedures described below. All animal experiments were approved by the cantonal veterinary offices of Zurich and Geneva.

Plasmids. eGFP-gephyrin encoding the P1 variant (11), gephyrin 3′UTR shRNA, and the control shRNA 3m (12) have been described previously. The remaining plasmids are presented in *SI Materials and Methods*.

Primary Neuron Cultures and Treatment. Primary rat embryonic hippocampal neuron culture preparation and transfection were done as described previously (30).

Antibodies and Immunohistochemistry. Immunocytochemistry of primary neuron cultures was performed as described earlier (31). The α2 subunit was stained in living cultures to ensure labeling of cell-surface receptors, followed by fixation, permeabilization, and detection of intracellular proteins. The antibodies are described in *SI Materials and Methods*.

Electrophysiology. Transfected hippocampal neurons (11 + 4 DIV) were recorded in the whole-cell voltage-clamp configuration at room temperature using a holding potential of −60 mV, as described in *SI Materials and Methods*. Nontransfected cells from the same dishes were used as mock control.

ACKNOWLEDGMENTS. We thank Prof. Angel De Blas (University of Connecticut, Storrs, CT) for kindly providing us with the gephyrin shRNA constructs, Prof. Jim Woodgett (Samuel Lunenfeld Research Institute, Ontario, Canada) for the GSK3β constructs, and Prof. Guenter Schwarz (University of Cologne, Cologne, Germany) for the bacterially expressed purified gephyrin. This work was supported by the Swiss National Science Foundation, the Forschungskredit of the University of Zurich, and the Hartmann-Müller Foundation.

1. Kim E, Sheng M (2004) PDZ domain proteins of synapses. *Nat Rev Neurosci* 5:771–781.
2. Fritschy JM, Harvey RJ, Schwarz G (2008) Gephyrin: Where do we stand, where do we go? *Trends Neurosci* 31:257–264.
3. Essrich C, Lorez M, Benson JA, Fritschy JM, Lüscher B (1998) Postsynaptic clustering of major $GABA_A$ receptor subtypes requires the γ 2 subunit and gephyrin. *Nat Neurosci* 1:563–571.
4. Feng G, et al. (1998) Dual requirement for gephyrin in glycine receptor clustering and molybdoenzyme activity. *Science* 282:1321–1324.
5. Tretter V, et al. (2008) The clustering of $GABA(_A)$ receptor subtypes at inhibitory synapses is facilitated via the direct binding of receptor α 2 subunits to gephyrin. *J Neurosci* 28:1356–1365.
6. Saiepour L, et al. (2010) Complex role of collybistin and gephyrin in $GABA_A$ receptor clustering. *J Biol Chem* 285:29623–29631.
7. Langosch D, Hoch W, Betz H (1992) The 93 kDa protein gephyrin and tubulin associated with the inhibitory glycine receptor are phosphorylated by an endogenous protein kinase. *FEBS Lett* 298:113–117.
8. Bausen M, Weltzien F, Betz H, O'Sullivan GA (2010) Regulation of postsynaptic gephyrin cluster size by protein phosphatase 1. *Mol Cell Neurosci* 44:201–209.
9. Kim MJ, et al. (2007) Synaptic accumulation of PSD-95 and synaptic function regulated by phosphorylation of serine-295 of PSD-95. *Neuron* 56:488–502.
10. Steiner P, et al. (2008) Destabilization of the postsynaptic density by PSD-95 serine 73 phosphorylation inhibits spine growth and synaptic plasticity. *Neuron* 60:788–802.
11. Lardi-Studler B, et al. (2007) Vertebrate-specific sequences in the gephyrin E-domain regulate cytosolic aggregation and postsynaptic clustering. *J Cell Sci* 120:1371–1382.
12. Yu W, et al. (2007) Gephyrin clustering is required for the stability of GABAergic synapses. *Mol Cell Neurosci* 36:484–500.
13. Chan SL, Mattson MP (1999) Caspase and calpain substrates: Roles in synaptic plasticity and cell death. *J Neurosci Res* 58:167–190.
14. Liu J, Liu MC, Wang KK (2008) Calpain in the CNS: From synaptic function to neurotoxicity. *Sci Signal* 1:re1.
15. Zadran S, Bi X, Baudry M (2010) Regulation of calpain-2 in neurons: Implications for synaptic plasticity. *Mol Neurobiol* 42:143–150.
16. Vinade L, Petersen JD, Do KQ, Dosemeci A, Reese TS (2001) Activation of calpain may alter the postsynaptic density structure and modulate anchoring of NMDA receptors. *Synapse* 40:302–309.
17. Lu X, Rong Y, Baudry M (2000) Calpain-mediated degradation of PSD-95 in developing and adult rat brain. *Neurosci Lett* 286:149–153.
18. Hawasli AH, et al. (2007) Cyclin-dependent kinase 5 governs learning and synaptic plasticity via control of NMDAR degradation. *Nat Neurosci* 10:880–886.
19. Kawasaki BT, Hoffman KB, Yamamoto RS, Bahr BA (1997) Variants of the receptor/channel clustering molecule gephyrin in brain: Distinct distribution patterns, developmental profiles, and proteolytic cleavage by calpain. *J Neurosci Res* 49: 381–388.
20. Hanna RA, Campbell RL, Davies PL (2008) Calcium-bound structure of calpain and its mechanism of inhibition by calpastatin. *Nature* 456:409–412.
21. Horne EA, Dell'Acqua ML (2007) Phospholipase C is required for changes in postsynaptic structure and function associated with NMDA receptor-dependent long-term depression. *J Neurosci* 27:3523–3534.
22. Gray NA, Zhou R, Du JZ, Moore GJ, Manji HK (2003) The use of mood stabilizers as plasticity enhancers in the treatment of neuropsychiatric disorders. *J Clin Psychiatry* 64(Suppl 5):3–17.
23. Moore GJ, et al. (2009) A longitudinal study of the effects of lithium treatment on prefrontal and subgenual prefrontal gray matter volume in treatment-responsive bipolar disorder patients. *J Clin Psychiatry* 70:699–705.
24. Wierenga CJ, Becker N, Bonhoeffer T (2008) GABAergic synapses are formed without the involvement of dendritic protrusions. *Nat Neurosci* 11:1044–1052.
25. Varoqueaux F, Jamain S, Brose N (2004) Neuroligin 2 is exclusively localized to inhibitory synapses. *Eur J Cell Biol* 83:449–456.
26. Graf ER, Zhang X, Jin SX, Linhoff MW, Craig AM (2004) Neurexins induce differentiation of GABA and glutamate postsynaptic specializations via neuroligins. *Cell* 119:1013–1026.
27. Poulopoulos A, et al. (2009) Neuroligin 2 drives postsynaptic assembly at perisomatic inhibitory synapses through gephyrin and collybistin. *Neuron* 63:628–642.
28. Kilman V, van Rossum MC, Turrigiano GG (2002) Activity deprivation reduces miniature IPSC amplitude by decreasing the number of postsynaptic $GABA_A$ receptors clustered at neocortical synapses. *J Neurosci* 22:1328–1337.
29. Prior P, et al. (1992) Primary structure and alternative splice variants of gephyrin, a putative glycine receptor-tubulin linker protein. *Neuron* 8:1161–1170.
30. Buerli T, et al. (2007) Efficient transfection of DNA or shRNA vectors into neurons using magnetofection. *Nat Protoc* 2:3090–3101.
31. Brünig I, Scotti E, Sidler C, Fritschy JM (2002) Intact sorting, targeting, and clustering of γ-aminobutyric acid A receptor subtypes in hippocampal neurons in vitro. *J Comp Neurol* 443:43–55.